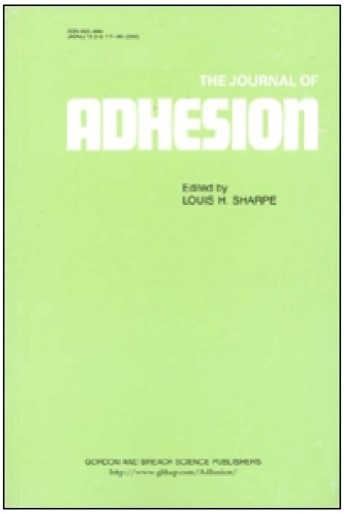

The Journal of Adhesion
Publication details, including instructions for authors and subscription information:
http://www.informaworld.com/smpp/title~content=t713453635

X-ray Photoelectron Spectroscopic Studies of the Bonding of Organic Monolayers on Various Oxidized Surfaces

H. R. Anderson Jr.[a]; J. D. Swalen[ab]
[a] IBM Research Laboratory, San Jose, California, U.S.A. [b] Polymer Science and Technology Department, IBM Systems Products Division, Junction, N.Y.

To cite this Article Anderson Jr., H. R. and Swalen, J. D.(1978) 'X-ray Photoelectron Spectroscopic Studies of the Bonding of Organic Monolayers on Various Oxidized Surfaces', The Journal of Adhesion, 9: 3, 197 — 211
To link to this Article: DOI: 10.1080/00218467808075114
URL: http://dx.doi.org/10.1080/00218467808075114

J. Adhesion, 1978, Vol. 9, pp. 197–211
© Gordon and Breach Science Publishers Ltd., 1978
Printed in Scotland

X-ray Photoelectron Spectroscopic Studies of the Bonding of Organic Monolayers on Various Oxidized Surfaces[†]

H. R. ANDERSON, Jr.[‡] and J. D. SWALEN
IBM Research Laboratory, San Jose, California 95193, U.S.A.

(*Received October 7, 1977*)
In Final Form February 27, 1978

With successive applications of one, three, and five monolayers of cadmium arachidate (cadmium eicosanoate) by the Langmuir–Blodgett technique to oxidized samples of indium, rhodium, silicon and tin, we observed progressive changes in the x-ray photoelectron spectral signals from the various elements both in the samples themselves and in the arachidate overlayers. With our APL computer program, all peaks were analyzed and fit to Gaussian curves with varying amplitudes and widths. Binding energies were thereby determined with high precision (± 0.05 eV), allowing us to infer some details about the interfacial region and molecular bonding. Differences in chemical shifts have been interpreted as arising from a partial transfer of charge, such as an acid–base interaction and the corresponding electrostatic force across the interface. Evidence is given to show that this force is localized within 2.5 nm of the interface.

INTRODUCTION

Because of their regular arrangement and known layer-to-layer spacing, monolayer assemblies of fatty acids and their salts have been used in a variety of ways to investigate intermolecular interactions and energy transfer.[1] We, in particular, have been utilizing these molecular layers for spectroscopic experiments on thin organic films and as such became interested in their intrinsic properties as well as their protective and overcoating properties. By

---

[†] Presented at the Borden Award Symposium honoring William A. Zisman during the National Meeting of the American Chemical Society in New Orleans, LA, March 21–25, 1977.

[‡] Now at IBM Systems Products Division, Polymer Science and Technology Department 49-F/Bldg 300–078, East Fishkill, Route 52, Hopewell Junction, N.Y. 12533.

x-ray photoelectron spectroscopy (XPS or ESCA) we embarked upon an investigation (1) to determine the concentrations of various species and (2) to observe any new species formation, particularly as a function of the number of monolayers. The interfacial region offers a rich environment for a whole host of chemical effects, such as structural changes, new compound formations, stoichiometric changes and even chemical changes at each stage of monolayer application.

Siegbahn *et al.*[2–4] have reported some early XPS results on layers of iodostearic acid and bromostearic acid on chromium plated brass. They found both (1) an increase in the iodine ($3d_{\frac{5}{2}}$) signal as more layers of iodostearic acid were added and (2) a decrease in the bromine ($3d_{\frac{3}{2},\frac{5}{2}}$) signal when the surface layers of bromostearic acid were covered with two layers of stearic acid.

We have done our XPS measurements on high purity oxidized surfaces on to which one, three, and five layers of cadmium arachidate were transferred from a water surface. These monolayers are well characterized films with thicknesses of 2.68 nm per layer and an area of 0.2 nm^2 per molecule, giving a close packed random stacking structure within the film. After careful and accurate computer analyses, significant changes with coverage were detected and chemically interpreted, the results of which we wish to report.

EXPERIMENTAL

Experiments were performed on films of indium, rhodium, silicon and tin with varying monolayer overcoats. The films of indium, rhodium, and tin

TABLE I

Process conditions for the various silicon oxide surfaces

	Oxidation conditions					Oxide characteristics	
	First oxidation step		Second oxidation step				
Sample	Temp. (°C)	Time in dry oxygen (min)	Time in steam (min)	Time in P-etch[a] (min)	Thickness (nm)	Refractive index	Location of hydroxyl groups
A	1200	58	—	0.15	45.3	1.475	Surface
B	1000	58	—	—	48.5	1.475	None
C	1000	5	4	—	58.0	1.475	Throughout

[a] See Ref. 5.

were prepared by electron beam evaporation by our thin film services and were plasma cleaned in oxygen and immersed in our water tank. The silicon samples studied were commercially available silicon wafers, p-type with a resistivity of 2 ohm cm, which were subjected to several oxidation conditions to produce oxide thicknesses of *ca.* 50 nm. Table I shows the various process conditions used to modify the hydroxyl content 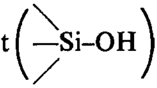 , i.e., acidity at the oxide surface. These were also cleaned in an oxygen plasma, leading to predominantly oxide surfaces on the silicon. XPS spectra showed mainly a single oxide peak, except for sample A where a weak additional peak could tentatively be assigned to a small amount of hydroxyl oxygens.

One, three, and five monolayers were transferred to the surfaces from a conventional Langmuir–Blodgett trough containing doubly distilled water buffered to a pH of 6.8 and with a 1 × 10^{-1} mol/m^3, concentration of cadmium chloride. Since the oxidized surfaces were hydrophilic, the substrates were first immersed in the trough, followed by a drop by drop addition of a chloroform solution of arachidic acid (eicosanoic acid, CH_3, $CH_3(CH_2)_{18}COOH$) to the surface to form a monolayer. Compression with a float, pulled by a force/length (two dimensional pressure) of approximately 30 mN/m, gave a uniform film on the water surface through which the substrates were slowly extracted and the first monolayer transferred. On each successive dipping and removal, two additional layers were added. Prior to the measurement of their XPS spectra, the samples were stored in a dust free environment.

TABLE II

Energies and mean free paths

Species	Internal standard eV	Electron kinetic energy eV	Mean free path in nm
In(3d$_{5/2}$)	445.52	1041	4.8±0.2
Sn(3d$_{5/2}$)	487.2	999	4.8±0.1
Si(2p)	103.6	1383	4.7±0.1
Rh(3d$_{5/2}$)	311.72	1175	4.2±0.3
C(1s)	284.3		

XPS spectra were obtained with a dispersion compensated monochromatized spectrometer (Hewlett-Packard Model 5950A) using Al(Kα) radiation. The electrical insulating properties of the films required the use of an electron emitting device ("flood gun") to avoid shifts and distortion of spectra; a flood gun current of 0.2 ma was found to give acceptable spectra.

The reported binding energies[6–8] for each film material were used as internal standards for low monolayer coverage (see Table II for our values). The differences between these internal standards and the C(1s) energy for all samples at three and five arachidate coverage were consistent for each material and allowed us to fix precisely the C(1s) binding energy at 284.3 eV which we adopted as our internal standard for high monolayer coverage. This is to be compared with the standard of 285 eV assigned to pump oil-contaminant-residual for C(1s).[9] It should be noted that the silicon signals were for oxidized silicon because of the relatively thick oxide overcoatings. For the other metals the signals originated from predominantly metallic environments.

ANALYSIS OF DATA

Each XPS curve was measured and digitized manually giving a series of points, viz., counts versus binding energy. These numbers were entered into an APL workspace for analysis as a Gaussian curve. The first and last ten points were separately averaged and an accurate base line was determined by linearly interpolating between these two end regions. The logarithms of counts (I) were then, by a least squares procedures, fit to a linear function of the binding energies squared, viz.,

$$\ln I_i = \ln A_i - c_i E_i^2,$$

where A_i is a constant giving peak height and c_i is a constant related to the inverse of the linewidth. The areas of the curves ($A_i\sqrt{\pi}/\sqrt{c_i}$), which are related to elemental compositions and cross-sections, agreed in all cases to within a few percent to a direct summation of the data points. It should be noted, however, that only points, approximately 30, around the maximum were used to determine the constants; noise near the baseline can make the corrected counts negative and their logarithms undefined. We were pleasantly surprised that the curves reproduced the data so well and only three constants were necessary to give accurate binding energy differences and areas. As an example, the average of the differences in binding energies between the Si(2s) peak and Si(2p) peak for all samples was 51.03 ± 0.04 eV.

Figures 1 and 2 show representative calculated Gaussian curves compared to the experimentally observed points as a function of uncorrected binding energy. The very good agreement of the line shape in detail gave us confidence in our analytical procedure. Corrections to the binding energies were made from the precisely determined centers of the peaks.

Although all the samples showed similar characteristics in their XPS spectra and will be detailed below, we will concentrate our discussion on one silicon sample as illustrative. In Figures 3–7 we see the attenuation of the photoelectron signals for O(1s) at 532.7 eV by successive layers of cadmium arachidate and concomitantly a new peak at 530.3 eV appears which is identified as arising from the carboxylic oxygen in the arachidate anion. At one monolayer this carboxylic oxygen signal appears as a shoulder on the low energy side (Figures 3 and 4) and at five monolayers the oxygen peak

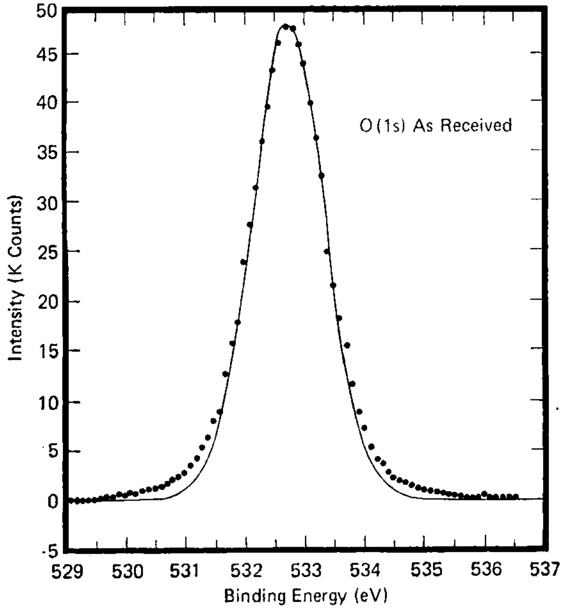

FIGURE 1 The XPS signal from O(1s) photoelectrons in K counts (points) for the oxidized sample C as received and before any surface treatment or coating and the theoretical curve from a least squares fit to the data points as a function of uncorrected binding energy.

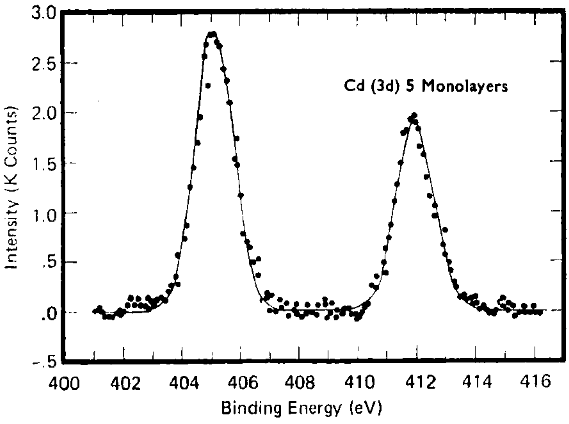

FIGURE 2 The XPS resonance from Cd(3d) with five monolayers of cadmium arachidate *vs.* binding energy.

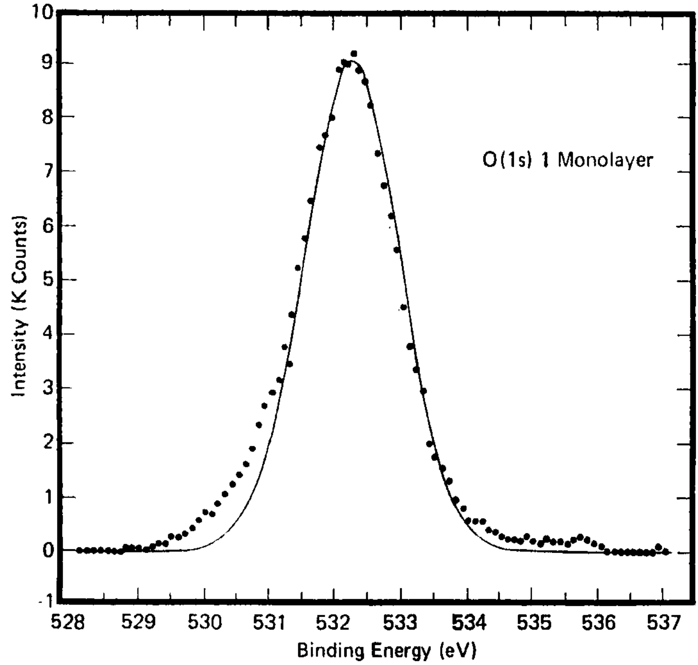

FIGURE 3 The XPS resonance of O(1s) in the sample C (oxidized silicon) *vs.* uncorrected binding energy. This signal is mainly from the oxygen in the silicon surface. The shoulder is from the carboxylic oxygen and is magnified in Figure 4.

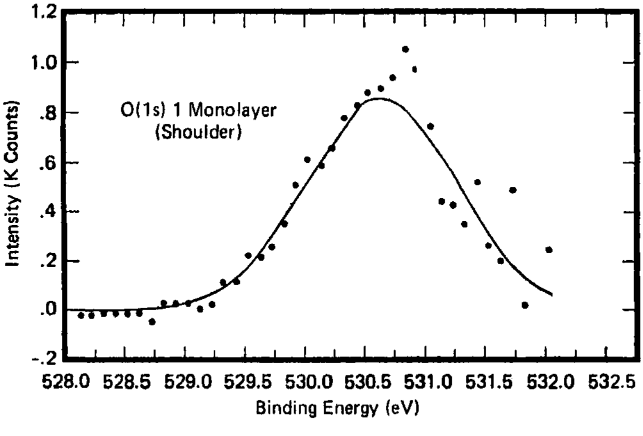

FIGURE 4 The difference in the experimental points and theoretical curve of Figure 3 here shown as the points, and compared to a theoretical curve shown as a line *vs.* uncorrected binding energy.

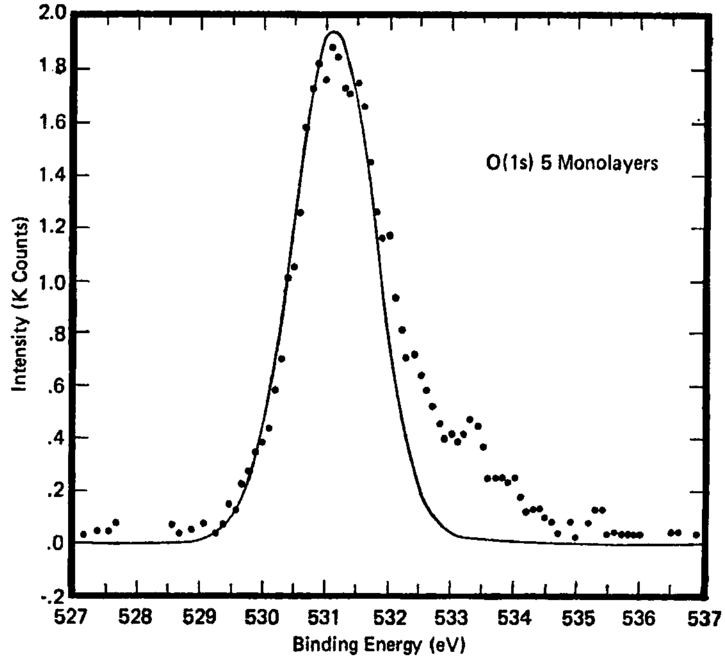

FIGURE 5 The XPS resonance from O(1s) in the sample C (oxidized silicon) with five monolayers *vs.* uncorrected binding energy. Notice the shoulder, which was the main peak of Figure 3, is now attentuated by the overlayers.

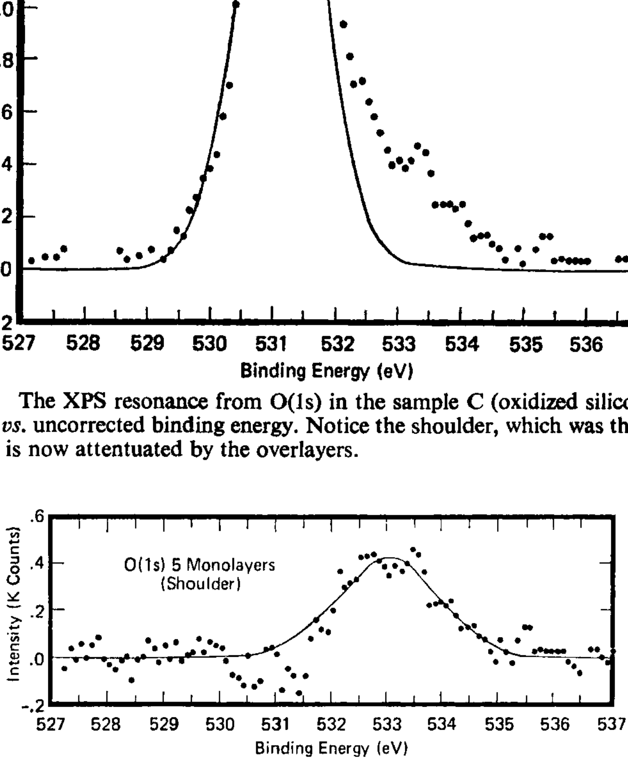

FIGURE 6 Theoretical fit to the shoulder of Figure 5, associated with the oxygen in the oxidized silicon layer.

arising from the underlying silicon oxide surface appears as a shoulder on the high energy side (Figures 5 and 6). At three monolayer coverage, the two curves have approximately the same intensity so that the total curve was fit and is shown in Figure 7. In the case of other substrates the double peak usually appeared at one monolayer coverage.

The series of curves (Figures 8 to 11) show the decay of the Si(2p) signal with increasing coverage. A semilog plot intensity versus thickness (Figure 12) gives a measure of the inelastic mean free path for photoelectrons from the slope. Similar decay curves[10] were found for various species in each sample and Table II lists our values. Although the mean free paths should scale according to the kinetic energy of the electrons (usually a simple power law or some more complicated function has been proposed,[11, 12]) the range in energy for our data is too small, considering the experimental accuracy of

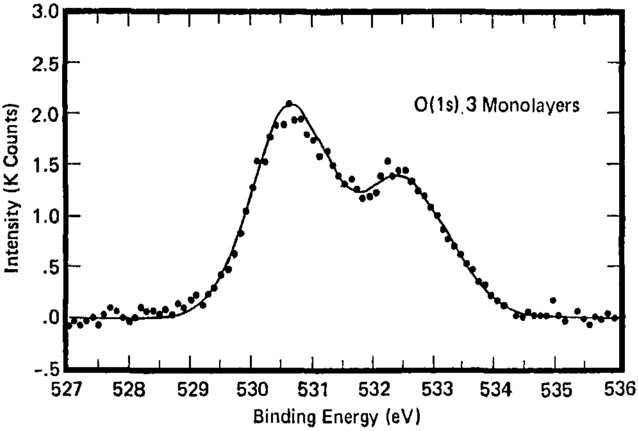

FIGURE 7 The XPS resonance from O(1s) in the sample C with three monolayers *vs.* uncorrected binding energy. Both types of oxygen appear at comparable intensity. The theoretical curve was obtained by successively varying the parameters because of convergence difficulties with the least squares procedure.

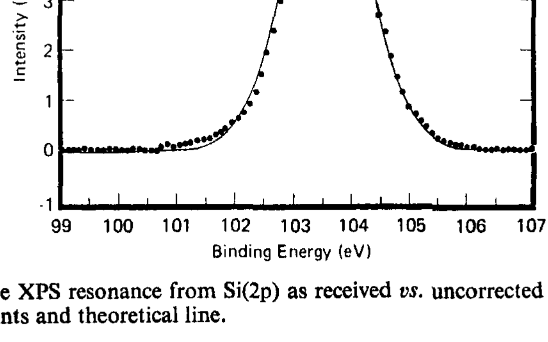

FIGURE 8 The XPS resonance from Si(2p) as received *vs.* uncorrected binding energy, experimental points and theoretical line.

our results, to see any trend. In spite of this, it is interesting that for comparable ranges of kinetic energy our values, *ca.* 4.6 nm, are in the low end of the range of values reported by Cadman *et al.*[13, 14] for a number of organic layers and slightly larger than those reported by Clark[15, 16] for a number of polymeric films. There is, however, no reason to expect arachidate layers to be exactly the same as other amorphous organic layers, especially with the usually higher density and pseudo ordering in the monolayer assemblies. As another comparison Flitsch and Raider[6] reported 2.7 ± 0.2 nm for silicon and 2.1 ± 0.5 mm for oxygen in an oxidized silicon sample.

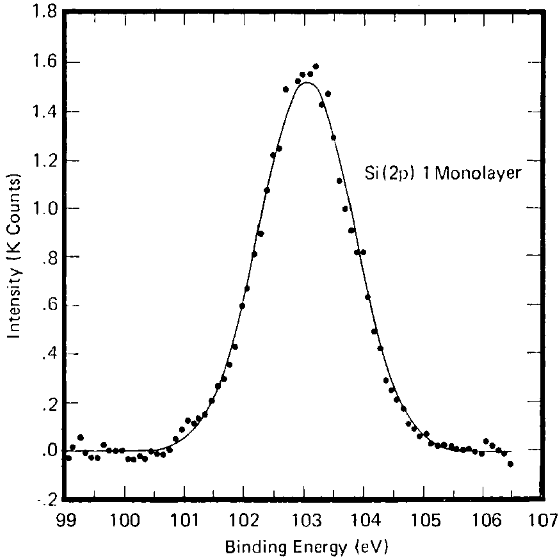

FIGURE 9 The XPS resonance from Si(2p) overcoated with one monolayer of cadmium arachidate *vs.* uncorrected binding energy.

Figure 12 also shows that carbon, carboxylic oxygen and cadmium signals all increase in intensity with increasing monolayer coverage. In comparing quantitatively the intensities of the signals from different atomic species or from just electrons from different shells of the same species, a number of factors have been identified by Powell[11] which must be considered. Since we cannot measure or monitor a number of instrumental factors, e.g., x-ray flux, electron optical factor, transmission of the analyzer, efficiency of the detector, and the geometrical factors relating to the area of irradiation and the acceptance angle of the detector, we have assumed that they all remain reasonably constant during the experiments and will approximately cancel when comparing ratios of intensities. A number of other factors, identified by Powell,[11] are, however, important and will be considered. The intensity of an

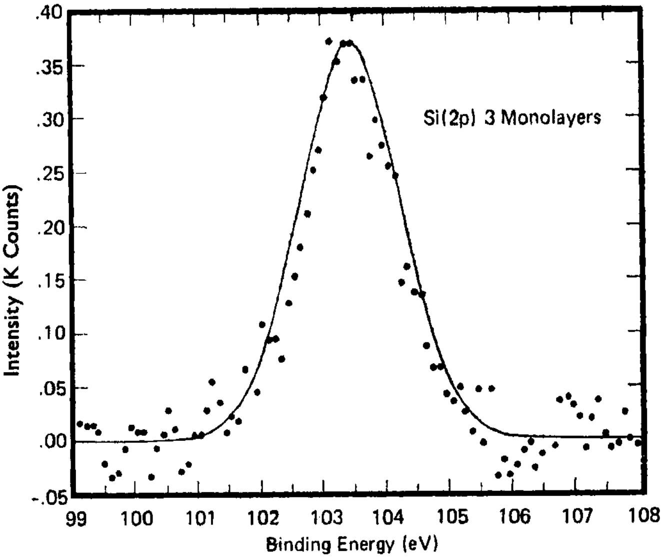

FIGURE 10 The XPS resonance from Si(2p) overcoated with three layers *vs.* uncorrected binding energy.

XPS signal ($I \propto N\sigma F\lambda(E)$) is proportional to the number density, N, of atoms of a given species, the total cross section for photoionization, σ, the angular asymmetry factor, F, and the inelastic mean free path, λ, which in turn is proportional to the kinetic energy (we used the 0.5 power).

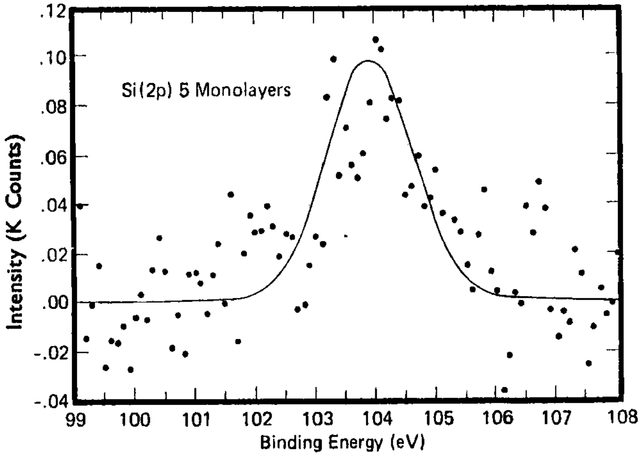

FIGURE 11 The XPS resonance from Si(2p) overcoated with five layers *vs.* uncorrected binding energy.

The ratio of the total cross-sections for photoionization of O(1s) to C(1s) was determined from the ratio of intensities of the arachidate carboxylic oxygen to that of the arachidate aliphatic carbon with three corrections: the initial carbon contamination was subtracted after attenuating it in each case for its depth from the surface; each carbon atom's contribution to the XPS signal, attenuated by its depth, was summed over the chains and each oxygen atom's contribution was also corrected for its location in the film; and the ratio of mean free paths was estimated from the square root of the ratio of the kinetic energies of the photoelectrons. No correction was necessary for the angular asymmetry factor because both signals involve 1s electrons. Our value for $\sigma(O(1s))/\sigma(C(1s))$ is 2.8 ± 0.5 and can be compared to ratios calculated from Wagner's[17] sensitivity values (2.5 by peak areas), from Joergenson and Berthou's[18] values (2.2), from NSBT's[19] values (2.7), and from Scofield's[20] theoretical values (2.93).

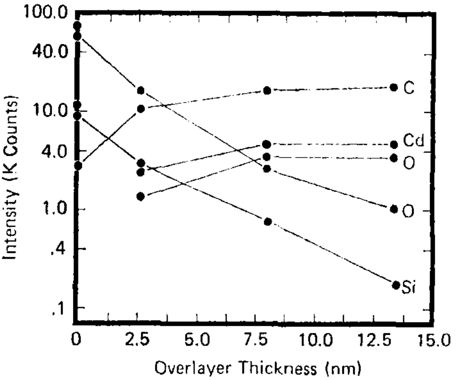

FIGURE 12 Intensity of the XPS signals *vs.* overlayer thickness in manometers. The decaying oxygen (O) curve is associated with the oxygen in the oxidized silicon. The increasing oxygen curve is associated with the carboxylic oxygen; we could not resolve the two different types of carboxylic oxygen species.

In comparing the ratio of the Cd($3d_{5/2}$) signal to the arachidate C(1s) signal (one cadmium ion per two arachidate chains), besides the corrections applied in the case of the O/C ratio, one must correct for the angular asymmetry factor. Using Powell's curves[11] for 3d electrons and 90° for the angle between the incident x-ray flux and the ejected photoelectrons, we calculate for cadmium $F(3d) = 1.32$. This is to be compared with the $F(1s) = 1.5$, which in this case of s electrons is independent of both atomic number and angle. Our intensity ratio for Cd($3d_{5/2}$) to C(1s), averaged over a number of five layer arachidate films on various substrates, gave us a ratio of cross sections of 13.5 ± 0.5. When we compare this to values calculated from Wagner's data[17] (13.3 to 15.8), from Joergenson and Berthou's data[18] (11.1), and from

Scofield's theoretical results[20] (11.95), we conclude that we have predominantly completely ionized acid and possibly even a small percentage of adsorbed cadmium ions from the monolayer tank. This is reasonable because most long chain aliphatic acids have a pK value of approximately 5 and at our pH of 6.8, one would predict about 98% ionization. X-ray work by

TABLE III

Differences in XPS binding energies in eV

Species	Number of monolayers	$O^{(M)}$–C‖	$O^{(A)}$–C	Cd–C		M–C			$C^{(C=O)}$–C
				$3d_{5/2}$	$3d_{3/2}$	3d		$3p_{3/2}$	
Indium	1	247.19	245.39	120.90	127.68	159.79		381.1	3.8
	3†	248.75	246.99	120.86	127.41	161.22		382.68	~3.2
	5	vw	246.69	120.60	127.31	160.94		vw	3.6
	Δ	−1.56	−1.45±0.2	0.2±0.1		−1.36±0.2			0.3±0.2
Tin	1	247.80	246.29	120.86	127.70	202.24	210.65	431.85	3.8
	3	248.46	246.78	120.58	127.29	203.09	211.49	432.92	3.5
	5	248.29	246.79	120.60	127.39	203.41	211.90	vw	3.5
	Δ	−0.58±0.1	−0.5±0.1	0.3±0.1		−0.85 to −1.2			0.3±0.1
								2p	
Silicon	1	248.01	246.41	120.97	127.70			−181.06	3.9
	3	248.40	246.58	120.61	127.14			−180.66	3.6
	5	248.34	246.58	120.53	127.36			−180.66	3.5
	Δ	−0.36±0.1	−0.17±0.1	0.4±0.1				−0.4±0.1	0.35±0.1
Rhodium	1	247.08§		120.80	127.51	23.00‡	27.80		3.8
	3	246.73		120.54	127.32	22.60	27.42		3.8
	5	246.53		120.53	127.33	23.17	28.41		3.7
	Δ	0.45±0.1		0.23±0.05		0±0.2			0.1±0.1

$\Delta = (1AA) - \frac{1}{2}(3AA + 5AA)$, where AA means arachidate monolayer.

† Two C(1s) signals were observed at an intensity ratio 2.5:1. The strong signal position was used in calculating differences. The weaker signal was 1.44 eV to higher energy and possibly could be identified with the aliphatic carbons of the first monolayer.

‡ A second doublet was observed, possibly rhodium oxide.

§ Only one oxygen signal was observed. Plasma cleaned samples also exhibited an oxygen peak at the same position as the arachidate oxygen peak. We conclude that both substrate and arachidate oxygen coincide and are superimposed.

‖ $O^{(M)}$ indicates the oxygens bonded to the metal surface.

$O^{(A)}$ indicates the oxygens bonded to the arachidate.

$C^{(C=O)}$ indicates the carbons bonded to the carbonyls of the carboxyl groups.

Ehlert,[21] on the other hand, reported for stearate films of barium, calcium and lead lower values (50–80%). Kuhn *et al.*[1] report x-ray results of Elsner where a cadmium concentration of 50% was found for the arachidate layers.

From our analyses the differences in binding energies of peak positions are given in Table III for each substrate covered by one, three, and five monolayers of cadmium arachidate. Differences were used to remove partially the influences of charging from the flood gun on the peak position. Since the C(1s) signal was strong, all the other peak positions have been related to it. From a perusal of the data in Table III, one immediately sees that the values for three and five monolayer coverage are quite similar, if not identical within experiment error, while those for one monolayer coverage are different, varying we contend in some relationship to the interaction at the substrate–monolayer interface compared to those between monolayers.

The carboxylic carbon appears as a weak, broad, featureless peak to higher energy than the aliphatic peak from the arachidate chain. Since charging would shift both carbon signals the same, the fact that the first chain carboxylic carbon is to even higher energy than those for the three and five layers indicates that it is behaving as an electron donor (Lewis base) with respect to the indium, tin and silicon oxide substrates. With the rhodium substrate, and as a matter of fact also with silver and gold substrates,[22] almost no shift differences were noted between the first layer and subsequent layers.

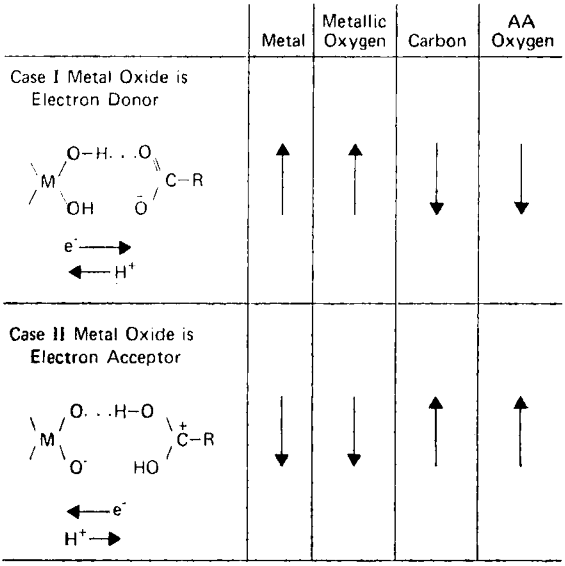

FIGURE 13 Schematic diagram showing the directions of binding energy shifts predicted on the basis of electron and proton transfer. If a partial valence electron is transferred, we infer that the core electrons associated with the donating species will be bound more tightly, and conversely.

Cadmium appears also to be involved in the interaction at the interface. A small shift to higher energy is seen. Both the substrate and the arachidate oxygen binding energy differences appear to follow approximately the metal signals. We tend to conclude that both types of oxygen, though at different binding energies, are in electrical contact with the grounded substrate. This is clear for the oxide layer, and the arachidate oxygen must also be in close proximity with the surface, i.e., bonded to the surface.

We interpret these facts related to the behavioral difference to mean that some extra chemical bonding is occurring between the first layer of cadmium arachidate and the substrate surface. There is probably some donor-acceptor charge transfer or, stating it another way, there is a Lewis acid–base interaction. Figure 13 shows schematically and qualitatively for electron and proton transfer how we would expect the binding energy to shift. On the basis of this crude model we identify the oxidized silicon, tin and indium surfaces as Lewis acids (electron acceptors) and rhodium may be a weak Lewis base (donor). Thus we have presented experimental evidence for additional electrostatic intermolecular forces at the interface formed by an organic overcoat on various oxidized surfaces. The strength of this force, which is related to the extent of the chemical shift or enthalpy of the chemical reaction, varied from substrate to substrate. These measurements also showed that electrostatic forces are operative within approximately 2.5 nm of the geometrical interface. This finding compares well with the independent assessment by Fowkes[23] using their metal–insulator–semiconductor (MIS) technique.

CONCLUSIONS

We believe that with careful experimental work and with our numerical procedures for the treatment of XPS data, one can extract fine details about interfacial phenomena, such as mean free paths for photoelectrons and chemistries at the surface. Admittedly the complete interpretation of the processes taking place at the interface is complicated by all the different intermolecular interactions and molecular species present. For example, the possibility of trapped water at the surface or in the films would influence the O(1s) signals. Channelling, island formation, changes in packing density of the first layer compared to subsequent layers, and additional adsorbed layers, to mention a few, would influence our reported values. Nevertheless, we feel that we have demonstratively shown that the first layer of cadmium arachidate chemically behaves differently from the adhesion between layers and that XPS can be used effectively to probe interfacial phenomena. The evaluation of individual chemical shifts provides insight into the chemical moieties in an organic molecule which give rise to an electrostatic force binding an organic coating to an oxide surface. It is our belief that careful XPS measurements with other monolayer species, such as long chain amines, alcohols, and fluorinated acids, and with other surfaces could further help with the methods here described to unravel and quantify acid–base properties and the related chemistry at interfaces.

Acknowledgements

We wish to thank R. Santo for the surface treatments and monolayer depositions. Without his careful work many of the fine details about the chemistry at the interface would have been lost or much more difficult to extract. We are grateful to W. A. Pliskin and C. R. Guarnieri for the preparation of the various substrates used in our monolayer studies. Discussions with C. R. Brundle, A. Dilks and J. M. Thomas are gratefully appreciated.

References

1. H. Kuhn, D. Möbius and H. Bücher, "Spectroscopy of Monolayer Assemblies", Chapter VIII, in *Physical Methods for Chemistry*, Vol. I, Part IIIB, A. Weissberger and B. W. Rossiter, Eds. (Wiley-Interscience, New York, 1972).
2. K. Larrson *et al.*, *Acta. Chem. Scand.* **30,** 2880 (1966).
3. K. Larrson *et al.*, *J. Coll. Interface Sci.* **29,** 268 (1960).
4. K. Siegbahn *et al.*, *Atomic, Molecular and Solid State Structure Studies by Means of Electron Spectroscopy* (Almquist and Wiksells, Uppsala, 1976).
5. W. A. Pliskin and R. P. Gnall, *J. Electro. Chem. Soc.* **111,** 872 (1964).
6. R. Flitsch and S. I. Raider, *J. Vac. Sci. Technol.* **12,** 305 (1975).
7. R. Nordberg *et al.*, *Inorg. Chem.* **9,** 2469 (1970).
8. J. M. Hill *et al.*, *Chem. Phys. Lett.* (to be published).
9. K. Siegbahn, D. A. Allison and J. H. Allison, "ESCA-Photoelectron Spectroscopy", in *Handbook of Spectroscopy*, J. W. Robinson, Ed. (C.R.C. Press, Cleveland, Ohio, 1974), Table 3, X-ray Core Spectra, pp. 517–749.
10. C. R. Brundle and J. D. Swalen have recently measured the attenuation of arachidate layers on four different gold films and a least squares fit to the data gave a mean escape depth of 4.5 ± 0.2 nm.
11. C. J. Powell, ASTM Symposium Volume on Quantitative Surface Analysis, to be published. See also C. J. Powell, *Surf. Sci.* **44,** 29 (1974).
12. K. Hirokawa and M. Oku, *Z. Anal. Chem.* **285,** 192 (1977).
13. P. Cadman *et al.*, *J. Chem. Soc. Faraday Trans. II*, **71,** 1777 (1975).
14. P. Cadman, G. Gossedge and J. D. Scott, *J. Electr. Spectr.* (in press) quote values for stearic acid and barium stearate by B. L. Henke and J. D. Andrade, respectively.
15. D. T. Clark, *Adv. in Polymer Science* **24** (Springer-Verlag, Berlin, Heidelberg and New York, 1977), pp. 125–188.
16. See *Faraday Discussions*, **60** (1975) for a discussion of the various mean free paths reported.
17. C. D. Wagner, *Anal. Chem.* **44,** 1050 (1972).
18. C. K. Joergenson and H. Berthou, *Fara. Disc. Chem. Soc.*, p. 269 (1972).
19. V. I. Nefedov, N. P. Serguishin, I. M. Band and M. B. Trzhaskovkaya, *J. Electr. Spectr.* **2,** 283 (1973) (referred to as NSBT).
20. J. H. Scofield, *J. Electr. Spectr.* **8,** 129 (1976).
21. R. C. Ehlert, *Adv. X-ray Anal.* **8,** 325 (1965).
22. C. R. Brundle, private communication.
23. F. M. Fowkes, private communication.